Article

Partitioning of diluted anyons reveals their braiding statistics

https://doi.org/10.1038/s41586-023-05883-2

Received: 30 September 2022

Accepted: 23 February 2023

Published online: 26 April 2023

Check for updates

June-Young M. Lee[1,4], Changki Hong[2,4], Tomer Alkalay[2,4], Noam Schiller[3], Vladimir Umansky[2], Moty Heiblum[2]✉, Yuval Oreg[3] & H.-S. Sim[1]✉

Correlations of partitioned particles carry essential information about their quantumness[1]. Partitioning full beams of charged particles leads to current fluctuations, with their autocorrelation (namely, shot noise) revealing the particles' charge[2,3]. This is not the case when a highly diluted beam is partitioned. Bosons or fermions will exhibit particle antibunching (owing to their sparsity and discreteness)[4–6]. However, when diluted anyons, such as quasiparticles in fractional quantum Hall states, are partitioned in a narrow constriction, their autocorrelation reveals an essential aspect of their quantum exchange statistics: their braiding phase[7]. Here we describe detailed measurements of weakly partitioned, highly diluted, one-dimension-like edge modes of the one-third filling fractional quantum Hall state. The measured autocorrelation agrees with our theory of braiding anyons in the time domain (instead of braiding in space); with a braiding phase of $2\theta = 2\pi/3$, without any fitting parameters. Our work offers a relatively straightforward and simple method to observe the braiding statistics of exotic anyonic states, such as non-abelian states[8], without resorting to complex interference experiments[9].

Fractional quantum Hall (FQH) systems host exotic quasiparticles (QPs), named anyons, that carry fractional charges and obey fractional statistics. An adiabatic braiding of abelian anyons leads to an added fractional statistical phase 2θ, whereas for non-abelian anyons, the original state transforms into another degenerate state[8,10,11]. The charge of the QPs can be determined by partitioning a full beam of QPs, leading to excess shot noise (autocorrelation of charge fluctuations)[2,3]. Here we demonstrate that partitioning a dilute anyon beam reveals the braiding phase of the QPs in the autocorrelation's Fano factor.

The traditional strategy to observe the statistics of QPs of FQH states involves interference in a Fabry–Pérot interferometer[12,13] or a Mach–Zehnder interferometer[14], where edge modes circulate localized QPs in the insulating bulk. Another recent approach[15] exploited a configuration of three quantum point contacts (QPCs) where two highly dilute beams, partitioned by two side QPCs, 'collided' at a central QPC (a typical Hong–Ou–Mandel configuration[16–18]). Measured for the anyonic one-third filling FQH state, the cross-correlation of the back-scattered QPs beams was interpreted as a partly anyonic bunching at the central QPC[15,19].

A different origin of the three-QPC outcome is based on time-domain braiding between the two impinging dilute anyon beams and the thermally (or vacuum) excited particle–hole anyon pairs at the central QPC[7,9]. To test this scenario, we focused on a two-QPC geometry where one QPC dilutes an anyon beam, further partitioned by a second QPC, resulting in excess shot noise (autocorrelation). Testing under different conditions, such as beam dilution, the second QPC's transmission and beam travel distance, we found an anomalous autocorrelation Fano factor ($\mathcal{F}_{\mathrm{dilute}}$) that agrees with our theory of time-domain braiding at the second (partitioning) QPC (without any fitting parameters).

Notably, although the theoretical description of the time-domain anyon braiding in a QPC is based on the chiral Luttinger liquid (CLL) theory (or the equivalent conformal field theory)[7,9], the saddle potential in the QPCs[20] is far from the ideal barrier in the CLL theory. To overcome this difficulty, we developed a theoretical description that hybridizes the CLL theory and a phenomenological theory in the spirit of the successful ubiquitous approach of charge determination via autocorrelation measurements[2,3].

Shot noise of full beam

Our experimental set-up is shown in Fig. 1a (Supplementary Note I). The source (S) is biased by voltage V_S, injecting a full QP beam with current $I_S = GV_S$, flowing chirally along Edge1, with conductance $G = \nu e^2/h$ at filling factor $\nu = 1/3$, where e is the electron charge and h is the Planck constant. The full beam is highly diluted by QPC1, with a reflection probability R_{QPC1} and thus current $I_{\mathrm{QPC1}} = I_S R_{\mathrm{QPC1}}$. The dilute beam flows chirally along Edge2, impinging at QPC2 (being 2 μm away), where it is further partitioned. The scattered current fluctuations are measured after being amplified by amplifiers A and B, with the spectral densities S_A, S_B and S_{AB} measured. The charge of the diluted QPs e^* was determined from the autocorrelation shot noise of QPC1[2,3,21–23]

$$S_{\mathrm{QPC1}} = 2e^* I_S R_{\mathrm{QPC1}}(1 - R_{\mathrm{QPC1}})\left[\coth\left(\frac{e^* V_S}{2k_B T}\right) - \frac{2k_B T}{e^* V_S}\right], \quad (1)$$

[1]Department of Physics, Korea Advanced Institute of Science and Technology, Daejeon, South Korea. [2]Braun Center for Submicron Research, Department of Condensed Matter Physics, Weizmann Institute of Science, Rehovot, Israel. [3]Department of Condensed Matter Physics, Weizmann Institute of Science, Rehovot, Israel. [4]These authors contributed equally: June-Young M. Lee, Changki Hong, Tomer Alkalay. ✉e-mail: moty.heiblum@weizmann.ac.il; hs_sim@kaist.ac.kr

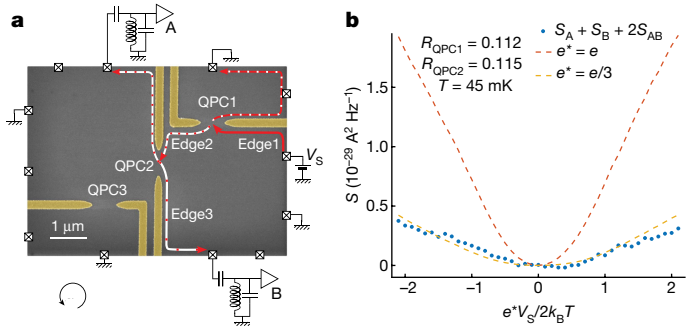

Fig. 1 | Partitioning diluted anyons in a two-QPC geometry. a, The experimental set-up. False-colour scanning electron microscope image with edge modes. The metallic gates of the QPC are coloured yellow. The ohmic contacts are more than 100 μm away from the core structure. The source current propagates along Edge1 and is diluted by QPC1 with R_{QPC1}. The diluted beam reaches QPC2 fabricated 2 μm away along Edge2. Partitioning takes place in QPC2 with back reflection along Edge3. The two amplifiers measure the excess autocorrelations and the cross-correlation. **b**, The spectral density of the noise generated by QPC1, with charge $e^* = e/3$ (blue dots, data; yellow dashed line, expected). It is obtained by a summation of the autocorrelations and cross-correlation of the current fluctuation in QPC2 diluted by QPC1 (Methods). Using this method, the injected QP charge towards QPC2 was found to be $e/3$. The experimental parameters are shown on the top left (detail in Supplementary Note II). The expected shot noise for a charge $e^* = e$ is shown for comparison (red dashed line).

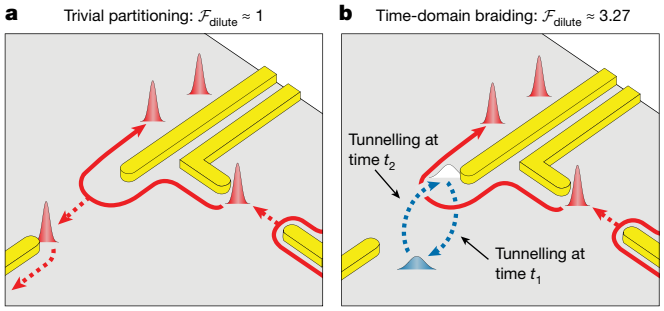

Fig. 2 | Trivial and braiding partitioning processes in QPC2. a, Trivial partitioning: QPC1 dilutes the incoming beam by reflection R_{QPC1} (red wavepackets), which is partitioned further in QPC2 by R_{QPC2}. Shot noise is proportional to $R_{QPC1}R_{QPC2}$. **b**, Time-domain braiding: QPC1 dilutes the incoming beam by reflection R_{QPC1} (red wavepackets). A thermally activated particle-like anyon, depicted by a blue wavepacket (leaving a hole, a white wavepacket) tunnels within QPC2 (blue arrow from one edge mode to another) at time t_1. The diluted anyon arrived (with probability R_{QPC1}). The particle anyon tunnels back at a later time t_2 (blue dashed arrows), thus braiding the arriving diluted anyon during the interval time t_2–t_1.

which was determined by $S_{QPC1} = S_A + S_B + 2S_{AB}$, with the electron temperature T and the Boltzmann constant k_B (Fig. 1b and Methods). The data agree well with equation (1) with $e^* = e/3$ (a similar measurement was performed with QPC2 (Supplementary Note II)).

We now elaborate on the phenomenological hybridization of the non-interacting expression in equation (1) and the interacting theory of the CLL. In the limit of very large V_S/T and very small R_{QPC1}, equation (1) agrees with the prediction of the CLL theory. In the CLL theory, the current and shot noise are expressed as $I_{QPC1} = e^*(W_{1\to2} - W_{2\to1})$ and $S_{QPC1} = 2e^{*2}(W_{1\to2} + W_{2\to1})$, where $W_{i\to j}$ is the tunnelling rate of an anyon from Edge$i$ to Edge$j$. When a full (undiluted) biased beam obeys $e^*V_S \gg k_BT$, the rate $W_{2\to1}$ is exponentially suppressed compared with $W_{1\to2}$, resulting in $S_{QPC1} = 2e^*I_{QPC1}$. The phenomenological binomial factor $(1 - R_{QPC1})$ in equation (1) relates to charge fluctuation of non-interacting particles in the QPC. The temperature-dependent term emanates from the detailed balance principle[22].

Time-domain braiding by diluted beam

We extend equation (1) to the two-QPC configuration. When a diluted beam is partitioned by QPC2, the spectral density S_{QPC2} of the excess autocorrelation of current fluctuations in QPC2 can be expressed as

$$S_{QPC2} = \mathcal{F}_{dilute} \times 2e^*I_{QPC1}R_{QPC2}(1 - R_{QPC2})\left[\coth\left(\frac{e^*V_S}{2k_BT}\right) - \frac{2k_BT}{e^*V_S}\right], \quad (2)$$

with $\mathcal{F}_{dilute}$ being dependent on the diluting R_{QPC1} of the beam (Supplementary Note III), and R_{QPC2} is the reflection probability of QPC2. This expression has the same structure as equation (1), with the replacement of I_S with I_{QPC1} and R_{QPC1} with R_{QPC2}. In the limit of large V_S and small R_{QPC2}, it becomes $S_{QPC2} = \mathcal{F}_{dilute} \times 2e^*I_{QPC2}$ with the current $I_{QPC2} = I_{QPC1}R_{QPC2}$. It is noted that for free fermions $\mathcal{F}_{dilute} = 1$.

The Fano factor $\mathcal{F}_{dilute}$ distinguishes between different partitioning processes. We consider the limits of large V_S and small R_{QPC2}, where $I_{QPC2} = e^*(W_{2\to3} - W_{3\to2})$, with spectral density $S_{QPC2} = 2e^{*2}(W_{2\to3} + W_{3\to2})$, and $\mathcal{F}_{dilute} = (W_{2\to3} + W_{3\to2})/(W_{2\to3} - W_{3\to2})$. Among possible partitioning processes, we first consider the trivial partitioning where an anyon in the dilute beam directly tunnels at QPC2 from Edge2 to Edge3 (Fig. 2a). This ubiquitous partitioning manifests particle antibunching[4–6], regardless of whether the particle is a boson, a fermion or an anyon. Here $\mathcal{F}_{dilute} = 1$ as the rate $W_{2\to3}$ exponentially dominates $W_{3\to2}$ at high enough voltage ($e^*V_S \gg k_BT$), in a similar fashion to the partitioning of a full beam.

However, the trivial partitioning process of a highly diluted anyonic beam with a high source voltage V_S leads to only a subdominant contribution to the observables. Instead, a more dominant process, which involves anyon braiding, takes place[7,9]. In this process, which we call time-domain braiding, the anyon that tunnels at QPC2 is not an arriving anyon of the dilute beam but a thermally (or virtually) excited anyon. The excited anyon tunnels between Edge2 and Edge3 (for example, from Edge2 to Edge3) at time t_1, leaving a hole behind (on Edge2). This anyon tunnels back at time t_2 and is 'pair annihilated' with the hole as long as $t_2 - t_1 \lesssim \hbar/k_BT$, where $\hbar$ is the reduced Planck constant. These probabilistic events of the particle–hole excitation and recombination form a loop in the time domain. The time-domain loop of the thermal anyon in QPC2 braids with the anyons in the diluted beam that arrive at QPC2 during the time interval t_2–t_1 (Fig. 2b), thus gaining a braiding phase (see below). The time-domain braiding dominates over the trivial partitioning as, according to the CLL theory, anyon tunnelling at a QPC becomes suppressed at higher energy. Within QPC2, anyon tunnelling for a thermal particle–hole pair excitation (with energy approximately k_BT) happens much more frequently than the tunnelling of an arriving diluted anyons (with energy approximately $e^*V_S \gg k_BT$, and required for the trivial partition).

Being fundamental in our experiment, we stress the time-domain braiding process again. The thermal particle–hole excitation happens at QPC2 between Edge2 and Edge3 either before (at t_1) or after (at t_2) the arrival of the diluted anyons at QPC2. These two subprocesses differ by an exchange phase, as the spatial order of the anyons (the thermal particle–hole and the arriving dilute anyons) on Edge2 differs between the subprocesses (Supplementary Fig. 9 and Supplementary Video 1). The interference between the subprocesses forms the time-domain loop of the thermal anyons that braids the diluted anyons. This braiding process leads to a modified Fano factor $\mathcal{F}_{dilute}$ (Methods and Supplementary Note III)

$$\mathcal{F}_{dilute} = -\cot\pi\delta\cot\left(\left(\frac{\pi}{2} - \theta\right)(2\delta - 1)\right) \approx 3.27, \quad (3)$$

when $R_{QPC1} \ll 1$. Here, δ is the scaling dimension of anyon tunnelling at QPC2, and 2θ ($\neq 0, 2\pi$) is the braiding angle. The value $\mathcal{F}_{dilute} = 3.27$ is obtained with the ideal $\nu = 1/3$ state, with the corresponding $\delta = 1/3$ and $\theta = \pi/3$.

As measuring the excess autocorrelation of a highly diluted beam is challenging, we developed a phenomenological theory for a moderately diluted beam. Going beyond the CLL theory, the critical step is the identification of the average braiding phase in the time-domain braiding process

$$\langle e^{2ik\theta}\rangle_{binomial} = \sum_{k=0}^{n} P_k e^{2ik\theta} = (1 - R_{QPC1} + R_{QPC1}e^{2i\theta})^n, \quad (4)$$

where k denotes the number of anyons in the dilute beam which arrive at QPC2 in the time interval $t_2 - t_1$. The phase term $e^{2ik\theta}$ corresponds to the braiding phase of a thermally excited anyon with each of the arriving anyons. The probability P_k of the k anyon event is naturally assumed to follow the binomial distribution $P_k = \frac{n!}{k!(n-k)!}(R_{QPC1})^k(1 - R_{QPC1})^{n-k}$, that is, the probability for k anyons being reflected by QPC1 with reflection probability R_{QPC1}. The maximum value of k is $n = I_S(t_2 - t_1)/e^*$. The average braiding phase is implemented in the calculation of $\mathcal{F}_{dilute}$ using the ideal CLL parameters (as above) and integrating over the time difference $t_2 - t_1$. As the beam is less diluted (that is, fuller), the trivial partitioning process is also considered in the above expression, although its contribution is small (Methods and Supplementary Note III). It is noted that the average braiding phase is $\langle e^{2ik\theta}\rangle_{binomial} = 1$ for fermions ($\theta = \pi$) and for bosons ($\theta = 0$).

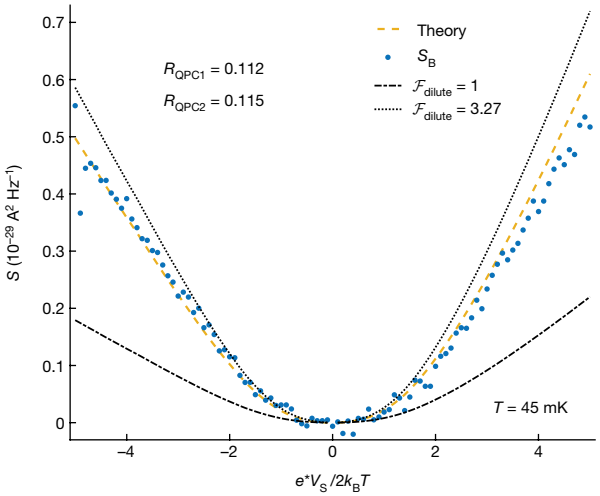

Fig. 3 | Excess autocorrelation noise as measured at amplifier B. A diluted beam of anyons is generated by reflection from QPC1 with probability $R_{QPC1} = 0.112$. The dilute beam impinges on QPC2 with $R_{QPC2} = 0.115$, creating excess autocorrelation (shot noise), shown by the blue dots. The yellow dashed line corresponds to the prediction of the phenomenological model given by equation (2), where $\mathcal{F}_{dilute}$ is calculated based on the measured R_{QPC1} (Supplementary Notes II and III). The black dotted line corresponds to the time-domain braiding process that dominates over the trivial process, with the Fano factor $\mathcal{F}_{dilute} = 3.27$ (in the dilute limit $R_{QPC1} \ll 1$). The black dashed line corresponds to $\mathcal{F}_{dilute} = 1$, namely, the predicted noise of trivial partitioning in QPC2.

Experimental results

We measured the excess spectral density S_B of the excess autocorrelation for two partitioning cases: injection of a full beam and injection of a dilute beam. We first performed these measurements in the integer regime (the outer edge mode of filling factor $\nu = 3$). The Fano factors in both cases agree with trivial partitioning $\mathcal{F}_{dilute} = 1$, with the expected electronic charge $e^* = e$ (Supplementary Note II). Similar measurements were performed at filling $\nu = 1/3$. Injecting a full beam led to S_B agreeing with equation (1) with charge $e^* \approx e/3$ (Supplementary Note II). Injecting a dilute beam, with $R_{QPC1}, R_{QPC2} \approx 0.1 \ll 1$, the experimental values of $\mathcal{F}_{dilute}$ were found close to $\mathcal{F}_{dilute} \approx 3.27$ (equations (3) and (4), and Fig. 3); ruling out the trivial process ($\mathcal{F}_{dilute} = 1$) and substantiating the time-domain braiding process. Here we utilized that S_B coincides with S_{QPC2} at large voltages (Supplementary Note IV).

In Fig. 4, the spectral density S_B of the autocorrelation was measured with varying dilutions, R_{QPC1}, and different partitioning, R_{QPC2}. With less dilution ('fuller' beam), the time-domain braiding process gives rise to smaller $\mathcal{F}_{dilute}$ and the trivial partitioning contribution to $\mathcal{F}_{dilute}$ is higher, albeit still small. Notice the excellent agreement between the experimental data and the phenomenological theory over a wide range of V_S/T, R_{QPC1} and R_{QPC2}, without fitting parameters. The deviation of the data from the theory at large V_S, compounded with less dilution (larger R_{QPC1}), is probably due to the variation of the QPC reflection with the source voltage V_S (not taken into account in the theory).

Time-domain braiding requires coherence between the two subprocesses[7,9]. The agreement between the experimental data and the theory with $2\theta = 2\pi/3$ and $\delta = 1/3$ in Figs. 3 and 4 implies that the inter-QPC distance of 2 μm is indeed shorter than the phase coherence length, and edge reconstruction[24] does not take place. To test this assumption, we fabricated a similar two-QPC geometry with an inter-QPC distance of 20 μm. In this case, the measured S_B showed a clear deviation from $\mathcal{F}_{dilute} \approx 3.27$, following the trivial formalism of equation (1) for non-interacting particles, with $R_{QPC1} \to R_{QPC1}R_{QPC2}$ (ref. 25; Fig. 5).

We extended our study to the fraction $\nu = 2/5$ (Supplementary Note V). Partitioning dilute anyons with $e^* = e/3$ (the outermost edge mode) at QPC2, we find a Fano factor close to $\mathcal{F}_{dilute} \approx 3.27$, which supports the time-domain braiding with $2\theta = 2\pi/3$ and $\delta = 1/3$ as in $\nu = 1/3$. However, partitioning with QPC2 the inner edge mode (conductance $e^2/15h$), carrying charge $e^* = e/5$, we found $\mathcal{F}_{dilute} \approx 1$, which is in our measurement's uncertainty ($R_{QPC1} = 0.088$ and $R_{QPC2} = 0.186$). The result is close to the Fano factor corresponding to the trivial partition process (see above).

Promise of time-domain braiding

It might be worthwhile to compare our two-QPC configuration with a recent work based on a three-QPC set-up[15]. In the latter work, the measured cross-correlation (of partitioned diluted 1/3-filling beams) agreed with quantum calculations[9,19], and was attributed to 'anyon bunching by collision' following a classical lattice model[19]. The collision is a different process from the time-domain braiding, providing only a subdominant contribution to the cross-correlation (similarly to trivial partitioning)[9]. In the collision process, two diluted anyons, injected from two side QPCs, simultaneously arrive at the central QPC and the presence of one anyon alters the tunnelling of the other one (at the central QPC) owing to anyonic bunching. Consequently, we tested our theory by performing a three-QPC experiment and found the results to agree well with our phenomenological approach (at a relatively large R_{QPC1}), supporting the underlying physics of the time-domain anyon braiding (Supplementary Note VI). Therefore, we believe that the previous three-QPC experimental results[15] should be regarded as time-domain braiding rather than anyon bunching. We note that two recent experiments also support the time-domain braiding process[26,27].

Here we demonstrate a relatively simple experimental configuration that identifies the statistical phase of abelian anyons in the FQH states. Our findings are also substantial considering the long-time disagreements between experiments (conductance and shot noise) and the chiral Luttinger theory[28]. For example, the theoretical voltage dependence of reflection probability in a QPC, $R_{QPC} \propto V^{2\delta-2}$, has not been confirmed experimentally (Supplementary Note II). As such, it is worth examining the robustness of our Fano factor, $\mathcal{F}_{dilute}$, with respect to a

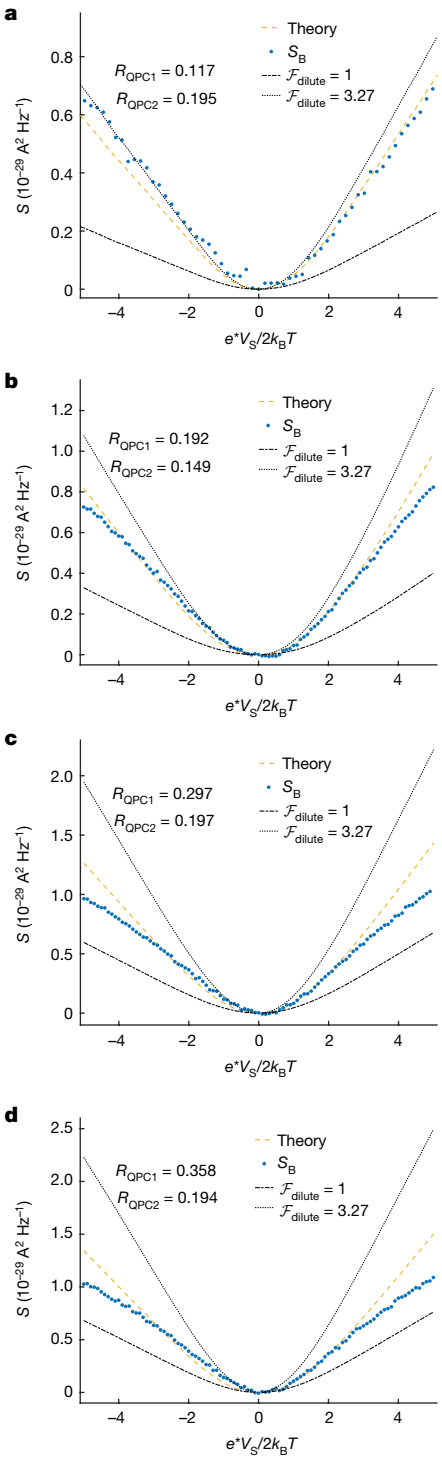

Fig. 4 | The dependence of the autocorrelation (amplifier B) on beam dilution (R_{QPC1}) and on R_{QPC2}. **a**–**d**, From more to less dilution via R_{QPC1}, with **a** R_{QPC1} = 0.117, **b** R_{QPC1} = 0.192, **c** R_{QPC1} = 0.297, and **d** R_{QPC1} = 0.358; excess autocorrelation (shot noise, blue dots) in the two-QPC configuration for different values of beam dilution. The yellow dashed lines are the theoretical predictions according to the phenomenological theory of equation (2). The black dashed lines are for the trivial process. The black dotted lines are for the dilute limit where the primary contribution to the noise results from the time-domain braiding process. The data are in a good agreement with the theory over a wide range of parameters. As predicted by equation (3), a higher dilution (smaller R_{QPC1}) minimizes the contribution of the trivial partitioning to the data, allowing the Fano factor of the autocorrelation to reach $\mathcal{F}_{dilute}$ = 3 . 27. See also Supplementary Fig. 5.

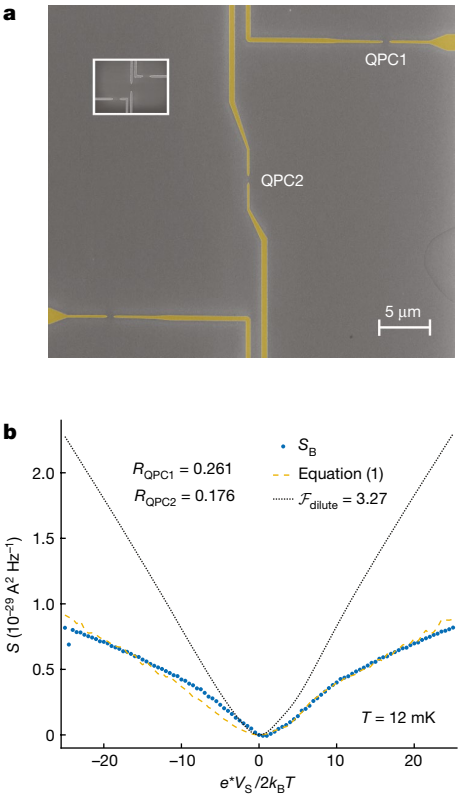

Fig. 5 | Two-QPC configuration with an inter-QPC distance of 20 μm. **a**, Scanning electron microscope image of the experimental set-up. The gates are marked in yellow. The 2-μm QPC separation structure is shown (for comparison) in the white-bordered inset. **b**, The blue dots are the measured excess autocorrelation with dilution of R_{QPC1} = 0.261 and R_{QPC2} = 0.176. The measurement results agree with the trivial model (that is, integer filling factor) in equation (1) with $R_{QPC1} \to R_{QPC1}R_{QPC2}$, suggesting energy loss and dephasing due to the long propagation distance. The black dotted line is the ideal anyonic behaviour with Fano factor $\mathcal{F}_{dilute}$ = 3.27.

variation in the scaling dimension δ. We find that $\mathcal{F}_{dilute}$ is expected to vary only by 10% throughout the range $1/3 < \delta < 2/3$ (Supplementary Note III).

Although it is natural to expect that a highly diluted particle beam, such as photons or electrons[4–6], exhibits single-particle scattering at a barrier, our work shows an exception to this expectation: impinging highly diluted fractional QPs undergo multi-particle scattering at a QPC constriction, as they are topologically linked (braided) with the time-domain trajectory of thermally excited anyons within the constriction. This feat is accomplished by a relatively simple two-QPC configuration—allowing a straightforward identification of the braiding phase in a considerably simpler method than interference experiments. Moreover, our work suggests a promising route towards observing the topological order of non-abelian anyons, such as in the 5/2 filling in the FQH regime[9].

Online content

Any methods, additional references, Nature Portfolio reporting summaries, source data, extended data, supplementary information, acknowledgements, peer review information; details of author contributions and competing interests; and statements of data and code availability are available at https://doi.org/10.1038/s41586-023-05883-2.

1. Hanbury Brown, R. & Twiss, R. Q. A test of a new type of stellar interferometer on Sirius. *Nature* **178**, 1046 (1956).
2. de-Picciotto, R. et al. Direct observation of a fractional charge. *Nature* **389**, 162 (1997).

3. Saminadayar, L. et al. Observation of the e/3 fractionally charged Laughlin quasiparticle. *Phys. Rev. Lett.* **79**, 2526 (1997).
4. Kimble, H. J., Dagenais, M. & Mandel, L. Photon antibunching in resonance fluorescence. *Phys. Rev. Lett.* **39**, 691 (1977).
5. Henny, M. et al. The fermionic Hanbury Brown and Twiss experiment. *Science* **284**, 296 (1999).
6. Oliver, W. D. et al. Hanbury Brown and Twiss-type experiment with electrons. *Science* **284**, 299 (1999).
7. Lee, B., Han, C. & Sim, H.-S. Negative excess shot noise by anyon braiding. *Phys. Rev. Lett.* **123**, 016803 (2019).
8. Nayak, C., Simon, S. H., Stern, A., Freedman, M. & Das Sarma, S. Non-abelian anyons and topological quantum computation. *Rev. Mod. Phys.* **80**, 1083 (2008).
9. Lee, J.-Y. M. & Sim, H.-S. Non-abelian anyon collider. *Nat. Commun.* **13**, 6660 (2022).
10. Leinaas, J. M. & Myrheim, J. On the theory of identical particles. *Nuovo Cimento B* **37**, 1 (1977).
11. Arovas, D., Schrieffer, J. R. & Wilczek, F. Fractional statistics and the quantum Hall effect. *Phys. Rev. Lett.* **53**, 722–723 (1984).
12. Nakamura, J. et al. Direct observation of anyonc braiding statistics. *Nat. Phys.* **16**, 931 (2020).
13. de C. Chamon, C., Freed, D. E., Kivelson, S. A., Sondhi, S. L. & Wen, X. G. Two point-contact interferometer for quantum Hall systems. *Phys. Rev. B* **55**, 2331–2343 (1997).
14. Kundu, H.K., Biswas, S., Ofek, N. et al. Anyonic interference and braiding phase in a Mach-Zehnder interferometer. *Nat. Phys.* **19**, 515–521 (2023).
15. Bartolomei, H. et al. Fractional statistics in anyon collisions. *Science* **368**, 6487 (2020).
16. Hong, C. K., Ou, Z. Y. & Mandel, L. Measurement of subpicosecond time intervals between two photons by interference. *Phys. Rev. Lett.* **59**, 2044 (1987).
17. Liu, R. et al. Quantum interference in electron collision. *Nature* **391**, 263 (1998).
18. Bocquillon, E. et al. Coherence and indistinguishability of single electrons emitted by independent sources. *Science* **339**, 1054 (2013).
19. Rosenow, B., Levkivskyi, I. P. & Halperin, B. I. Current correlations from a mesoscopic anyon collider. *Phys. Rev. Lett.* **116**, 156802 (2016).
20. Chung, Y. C. et al. Anomalous chiral Luttinger liquid behavior of diluted fractionally charged quasiparticles. *Phys. Rev. B* **67**, 201104(R) (2003).
21. Heiblum, M. Fractional Charge Determination via Quantum Shot Noise Measurements, in *Perspectives of Mesoscopic Physics: Dedicated to Yoseph Imry's 70th Birthday* (eds Ahrony, A. & Entin-Wohlman, O.) 115–136 (World Scientific, 2010).
22. Feldman, D. E. & Heiblum, M. Why a noninteracting model works for shot noise in fractional charge experiments. *Phys. Rev. B* **95**, 115308 (2017).
23. Trauzettel, B., Roche, P., Glattli, D. C. & Saleur, H. Effect of interactions on the noise of chiral Luttinger liquid systems. *Phys. Rev. B* **70**, 233301 (2004).
24. Rosenow, B. & Halperin, B. I. Nonuniversal behavior of scattering between fractional quantum Hall edges. *Phys. Rev. Lett.* **88**, 096404 (2002).
25. Blanter, Y. M. & Büttiker, M. Shot noise in mesoscopic conductors. *Phys. Rep.* **336**, 1–116 (2000).
26. Glidic, P. et al. Cross-correlation investigation of anyon statistics in the $\nu = 1/3$ and 2/5 fractional quantum Hall states. *Phys. Rev. X* **13**, 011030 (2023).
27. Ruelle, M. et al. Comparing fractional quantum Hall Laughlin and Jain topological orders with the anyon collider. *Phys. Rev. X* **13**, 011031 (2023).
28. Glattli, D. C. Tunneling Experiments in the Fractional Quantum Hall Effect Regime in *The Quantum Hall Effect* Progress in Mathematical Physics Vol 45 (eds Douçot, B. et al.) 163–197 (Birkhäuser, 2005).

Methods

Theory of the Fano factor

In the CLL theory and the equivalent conformal field theory[9], the time-domain braiding process is described by a non-equilibrium correlator $C_{\mathrm{neq}}(t_1, t_2)$ of the anyon tunnelling operator at QPC2 in the presence of a dilute anyon beam impinging at QPC2. It is expressed as $C_{\mathrm{neq}}(t_1, t_2) = \langle e^{2ik\theta}\rangle_{\mathrm{Poissonian}} C_{\mathrm{eq}}(t_1, t_2)$ in the limit of a highly diluted beam, namely, $R_{\mathrm{QPC1}} \ll 1$, where $C_{\mathrm{neq}}(t_1, t_2)$ is the equilibrium correlator in the absence of the dilute beam. Here, $\langle e^{2ik\theta}\rangle_{\mathrm{Poissonian}} = \sum_{k=0}^{\infty} Q_k e^{2ik\theta}$ is the average of the braiding phase $e^{2ik\theta}$, which accumulates when the time-domain loop of thermally excited anyons braids with k anyons of the dilute beam arriving at QPC2 in the time interval $t_2 - t_1$. The probability Q_k represents k random anyon injections from Edge1 to Edge2 at QPC1 (Figs. 1 and 2) over the time interval $t_2 - t_1$. For a highly diluted beam the Poisson distribution is $Q_k = (m^k/k!)e^{-m}$, where $m = I_{\mathrm{QPC1}}(t_2 - t_1)/e^*$.

It is naturally expected that in a less dilute ('fuller') beam (with a relatively large R_{QPC1}, yet small enough for anyon tunnelling), the distribution of anyons in the beam follows a binomial distribution rather than the Poissonian distribution. Hence, to describe the cases of less dilute beams, we replace the multiplicative factor $\langle e^{2ik\theta}\rangle_{\mathrm{Poissonian}}$ by the average braiding phase $\langle e^{2ik\theta}\rangle_{\mathrm{binomial}}$, with the latter averaged over the binomial distribution in equation (4). Then the correlator is

$$C_{\mathrm{neq}}(t_1, t_2) = \left(1 - R_{\mathrm{QPC1}} + R_{\mathrm{QPC1}} e^{2i\theta \mathrm{sign}(t_2 - t_1)}\right)^{\frac{I_S}{e^*}|t_1 - t_2|} C_{\mathrm{eq}}(t_1, t_2). \quad (5)$$

In the dilute limit of $R_{\mathrm{QPC1}} \ll 1$, the multiplicative factor $(1 - R_{\mathrm{QPC1}} + R_{\mathrm{QPC1}} e^{\pm 2i\theta})^{\frac{I_S}{e^*}|t_1 - t_2|}$ is reduced to the factor $e^{-(1 - e^{\pm 2i\theta})\frac{I_{\mathrm{QPC1}}}{e^*}|t_1 - t_2|}$ found in a previous work[9]. Employing $C_{\mathrm{neq}}(t_1, t_2)$ with an integral over $t_2 - t_1$, it is straightforward to compute the rates of anyon tunnelling (back and forth) at QPC2 in the time-domain braiding process. At zero temperature and $R_{\mathrm{QPC2}} \ll 1$, we get

$$\begin{aligned} W_{2\to3}^{\mathrm{braid}} &\propto \mathrm{Re}[e^{i\pi\delta}(-\log(1 + R_{\mathrm{QPC1}}(e^{-i2\theta} - 1)))^{2\delta - 1}], \\ W_{3\to2}^{\mathrm{braid}} &\propto \mathrm{Re}[e^{i\pi\delta}(-\log(1 + R_{\mathrm{QPC1}}(e^{-i2\theta} - 1)))^{2\delta - 1}], \end{aligned} \quad (6)$$

with the full expressions given in Supplementary Note III. In contrast to the trivial process where $W_{3\to2}$ is exponentially suppressed compared with $W_{2\to3}$, both $W_{2\to3}^{\mathrm{braid}}$ and $W_{3\to2}^{\mathrm{braid}}$ are non-negligible in the time-domain braiding. The appearance of the combination $(e^{\pm i2\theta} - 1)$ in equation (6) implies that the rates $W_{2\to3}^{\mathrm{braid}}$ and $W_{3\to2}^{\mathrm{braid}}$ vanish, and thus do not contribute to the tunnelling currents and noise at QPC2 in the cases of fermions ($\theta = \pi$) or bosons ($\theta = 0$). Hence the time-domain braiding does not exist with fermions or bosons, but only with anyons[29–32].

When the time-domain braiding process dominates over other processes, the Fano factor is written as

$$\begin{aligned} \mathcal{F}_{\mathrm{dilute}} &= \frac{W_{2\to3}^{\mathrm{braid}} + W_{3\to2}^{\mathrm{braid}}}{W_{2\to3}^{\mathrm{braid}} - W_{3\to2}^{\mathrm{braid}}} \\ &= -\cot\pi\delta \frac{\mathrm{Re}[(-\log(1 + R_{\mathrm{QPC1}}(e^{-i2\theta} - 1)))^{2\delta - 1}]}{\mathrm{Im}[(-\log(1 + R_{\mathrm{QPC1}}(e^{-i2\theta} - 1)))^{2\delta - 1}]}. \end{aligned} \quad (7)$$

In the dilute limit of $R_{\mathrm{QPC1}} \ll 1$, we find $\mathcal{F}_{\mathrm{dilute}} \to -\cot\pi\delta \frac{\mathrm{Re}[(1 - e^{-i2\theta})^{2\delta - 1}]}{\mathrm{Im}[(1 - e^{-i2\theta})^{2\delta - 1}]}$ as in equation (3). That zero-temperature value of $\mathcal{F}_{\mathrm{dilute}}$ of the two-QPC set-up corresponds to the Fano factor of the cross-correlation of a three-QPC set-up predicted in refs. 9,19. As the beam becomes less dilute ('fuller'), the trivial partitioning process contributes more to the rates of $W_{2\to3}^{\mathrm{triv}}$ and $W_{3\to2}^{\mathrm{triv}}$ (Supplementary Note III). Then the Fano factor $\mathcal{F}_{\mathrm{dilute}}$ is obtained according to all the rates accounted for all the processes, $W_{2\to3} = W_{2\to3}^{\mathrm{braid}} + W_{2\to3}^{\mathrm{triv}}$ and $W_{3\to2} = W_{3\to2}^{\mathrm{braid}} + W_{3\to2}^{\mathrm{triv}}$, with the experimentally measured R_{QPC1} as input of the calculation. We note that $W_{2\to3}^{\mathrm{triv}}$ and $W_{3\to2}^{\mathrm{triv}}$ are not negligible but much smaller than $W_{2\to3}^{\mathrm{braid}}$ and $W_{3\to2}^{\mathrm{braid}}$ for the values of R_{QPC1} studied in our experiments.

It should be noted that partitioning a non-diluted beam can provide an anyonic signature through a different process from our partitioning a strongly diluted beam[33].

Obtaining S_{QPC1} in a two-QPC configuration

While performing the two-QPC measurements, the noise generated by QPC1 (S_{QPC1}) is not directly accessible (owing to the locations of the amplifiers). However, current conservation can be used to relate S_{QPC1} to the correlations measured in the experiment. By current conservation in QPC2

$$I_{\mathrm{QPC1}} = I_{\mathrm{QPC2}}^{\mathrm{A}} + I_{\mathrm{QPC2}}^{\mathrm{B}},$$

where I_{QPC1} is the dilute current generated by QPC1 and $I_{\mathrm{QPC2}}^{\mathrm{A/B}}$ is the output current of QPC2 that reaches amplifier A/B (Fig. 1a). The same relation also holds for the averages

$$\langle I_{\mathrm{QPC1}}\rangle = \langle I_{\mathrm{QPC2}}^{\mathrm{A}}\rangle + \langle I_{\mathrm{QPC2}}^{\mathrm{B}}\rangle.$$

Subtracting these two equations and taking the square we arrive at a relation between the current correlations

$$S_{\mathrm{QPC1}} = S_{\mathrm{A}} + S_{\mathrm{B}} + 2S_{\mathrm{AB}},$$

which allows us to obtain S_{QPC1} by summing the autocorrelations (S_{A} and S_{B}) and the cross-correlation (S_{AB}) measured in the experiment.

Data availability

Source data are provided with this paper. All other data related to this paper are available from the corresponding authors upon reasonable request.

29. Han, C., Park, J., Gefen, Y. & Sim, H.-S. Topological vacuum bubbles by anyon braiding. *Nat. Commun.* **7**, 11131 (2016).
30. Lee, J.-Y. M., Han, C. & Sim, H.-S. Fractional mutual statistics on integer quantum Hall edges. *Phys. Rev. Lett.* **125**, 196802 (2020).
31. Morel, T., Lee, J.-Y. M., Sim, H.-S. & Mora, C. Fractionalization and anyonic statistics in the integer quantum Hall collider. *Phys. Rev. B* **105**, 075433 (2022).
32. Jonckheere, T., Rech, J., Grémaud, B. & Martin, T. Anyonic statistics revealed by the Hong–Ou–Mandel dip for fractional excitations. Preprint at https://arxiv.org/abs/2207.07172 (2022).
33. Safi, I., Devillard, P. & Martin, T. Partition noise and statistics in the fractional quantum Hall effect. *Phys. Rev. Lett.* **86**, 4628 (2001).

Acknowledgements J.-Y.M.L. acknowledges support from Korea NRF, NRF-2019-Global PhD fellowship. H.-S.S. acknowledges support from Korea NRF, the SRC Center for Quantum Coherence in Condensed Matter (grant number 2016R1A5A1008184 and RS-2023-00207732). N.S. acknowledges discussions with Y. Shapira and A. Stern, and acknowledges the Clore Scholars Programme. Y.O. acknowledges the partially supported by grants from the ERC under the European Union's Horizon 2020 research and innovation programme (grant agreements LEGOTOP No. 788715 and HQMAT No. 817799), the DFG (CRC/Transregio 183, EI 519/7-1), the BSF and NSF (2018643), and the ISF Quantum Science and Technology (2074/19). M.H. acknowledges the continuous support of the Sub-Micron Center staff, the support of the European Research Council under the European Community's Seventh Framework Program (FP7/2007-2013)/ERC under grant agreement number 713351. We thank G. Fève, F. Pierre and C. Mora for discussions.

Author contributions J.-Y.M.L. and H.-S.S. developed the theory and analysed the data. C.H. and T.A. fabricated the structures, did all measurements and analysed the data. N.S. and Y.O. added perspective on the theory. V.U. designed and grew the heterostructures by Molecular Beam Epitaxy. M.H. supervised the experiments.

Competing interests The authors declare no competing interests.

Additional information

Supplementary information The online version contains supplementary material available at https://doi.org/10.1038/s41586-023-05883-2.

Correspondence and requests for materials should be addressed to Moty Heiblum or H.-S. Sim.

Peer review information *Nature* thanks the anonymous reviewers for their contribution to the peer review of this work. Peer reviewer reports are available.